Energy Transfer in Li*(3p)−H_2 Collisions

Solomon Bililign*,† and Brian C. Hattaway
Department of Physics, North Carolina A&T State University, Greensboro, North Carolina 27411

Neri Geum
Department of Chemistry, Dankook University, Cheonan 330-714, South Korea

Gwang-Hi Jeung*,‡
Laboratoire Aimé Cotton (Bât. 505) and ASCI (Bât.506), Campus d'Orsay, 91405 Orsay, France

Received: June 12, 2000; In Final Form: August 24, 2000

The direct collisional energy transfer process Li*(3p) + H_2 → Li*(3s) + H_2 is investigated under gas cell conditions. In particular, we measured the nonreactive far-wing absorption profile of LiH_2 complexes by monitoring the Li(3s) → Li(2p) fluorescence at 812.6 nm. Strong satellite structures are observed at around 700 cm^{-1} in the blue wing and 162 cm^{-1} in the red wing of the LiH_2 profile. The experimental results are in agreement with ab initio theoretical predictions, which showed a strong probability of a diabatic transition making the 3p−3s quenching easy.

I. Introduction

The energy transfer in collisions between excited state alkali-metal atoms and rare-gas atoms has been extensively studied;[1−4] however, the nonreactive quenching by H_2 has been much less investigated. It has been shown in many cases that the nonreactive quenching cross section for H_2 is significantly larger than those for rare-gas atoms. This is a result of the existence of additional energy transfer pathways.[5,6]

The collisions of alkali atoms with molecular hydrogen leading to a nonreactive inelastic scattering or a reactive collision leading to the formation of metal hydride have been subjects of intensive research over the last two decades.[7−10] They represent the simplest three-body problems and have been a very useful testing ground for a nonadiabatic process and other dynamical models.

The "half-collision" pump−probe technique to measure the continuum or "scattering state" absorption profiles of M−H_2 collision complex has been used for a number of metal atom reagents.[11−15] In this technique, the pump laser excites the transient collision complex directly from the ground state potential energy surface to an excited potential energy surface. This is followed by the second half of the reaction process, reaction on the excited surface. The products can then be measured state selectively by laser-induced fluorescence (LIF). The technique allows selective excitation of states of well-defined symmetry in the collision complex. Final state-resolved measurement of the far-wing action spectra are sensitive both to the shape of the quasimolecular potential energy surface in the reactive entrance channel and to the subsequent dynamical evolution of the excited state. This provides information on nuclear reaction dynamics, nonadiabatic interactions, and the effect of reagent electronic orbital alignment on the final state branching and energy disposal.

A large number of studies have been conducted on the collisional quenching, fine structure changing collisions, and far-wing absorption studies of excited states of Li($2p^2P_j$) state with rare gases.[16−19] However, very little has been learned about the system involving the possibly reactive hydrogen molecule instead of the noble gas atoms.[20]

Our recent work[21] showed that the Li(2p)−H_2 collision pairs have enough kinetic energy to overcome the energy insufficiency at about 600 °C to form LiH. Theoretical studies[22] have also suggested that LiH can be produced via a potential energy surface hopping using the diabatic coupling. The reaction involves a stable C_{2v} intermediate ($2^2A'$) where the initial collision energy would be redistributed into the internal vibrations before the LiH bond is formed and H−H bond is broken. As the surface crossing point lies lower than the Li(2p) + H_2 asymptote the required kinetic energy is just the endothermicity of the reaction.

We have recently observed the formation of LiH from the Li(3p) + H_2 reaction when the pump laser is tuned near the resonant energy of the Li(3p−2s).[23] In these studies we have observed the efficient formation of LiH and we have experimentally demonstrated that secondary collisions can be ruled out under the conditions of this experiment since the observed signals are linear in H_2 pressure in the range of 4−10 Torr of H_2, and nearly independent of pump−probe delay time at 10 Torr of H_2 over the range of 5−12 ns. Measurements at higher pressure of H_2 do show a contribution from multiple collision processes evidenced by an increase in signal with pump−probe delay time. The signals are also nearly linear in Li pressure observed by changing the oven temperature from 500 to 600 °C. Our theoretical calculations have shown the existence of stable intermediates for this state and their equilibrium geometries are not linear but bent (C_{2v}). In the far-wing studies, the LiH signal disappeared as soon as we tuned further to the near red-wing ($\Delta \approx -160$ cm^{-1}) and reappeared again when the laser is tuned in the far red wing ($\Delta < -200$ cm^{-1}). To understand the lack of reaction product in these red-wing scattering experiments, we used the half-collision approach to study the process:

* Authors to whom correspondence should be addressed.
† E-mail: Bililign@ncat.edu. Fax: (336)-334−7423.
‡ E-mail: jeung@asci.fr.

10.1021/jp0020992 CCC: $19.00
Published on Web 09/29/2000

$$Li(2s\ ^2S) + H_2 + h\nu \rightarrow [Li(3p)H_2]^* \rightarrow Li(3s) + H_2 \quad (1)$$

The collisional energy transfer for the LiH_2 system was studied by observing the atomic fluorescence on the Li(3s−2p) transition. In this work no attempt was made to distinguish between the possible mechanisms to populate the Li*(3s) state: radiative decay from the 3p state, or direct collisonal quenching of the LiH_2 complex into the 3s state. The collisional quenching process is analogous to predissociation of the complex.

Ab initio theoretical calculations of the relevant potential energy surfaces are performed independently and are used to expalin the observed experimental results.

II. Experimental Details

The experimental setup is similar to the one described in previous works.[12−15] Briefly, the doubled and tripled frequencies of a 20-Hz Nd:YAG laser were used to pump two dye lasers simultaneously in a laser pump−probe arrangement. The pump dye laser was operated using a DCM dye whose output is frequency doubled to the spectral region of the Li(2s−3p) second resonance transition at 323.3 nm. The pump laser pulse had a typical pulse width of 4−6 ns and pulse energy of 200 μJ. This output was focused to the center of a five-arm stainless steel heat pipe oven containing Li vapor and the quenching gas (H_2) at an oven temperature of 900 K, corresponding to Li atom vapor density of $\sim 10^{13}/cm^3$. Typical operating pressure of the buffer gas (H_2) was 10 Torr, and the pressure was measured with a capacitance manometer. The fluorescence is collected using a lens and a steering mirror assembly by a 35 mm McPherson monochromator operated with wide slits. The fluorescence is detected with a cooled photomultiplier, and the signal output is amplified using a fast preamplifier and analyzed using a gated integrator/boxcar averager system.

In this experiment we attempted to measure both the direct atomic fluorescence from the laser excited Li*($3p^2P$) state to the ground state and the cascade fluorescence of the Li(3s−2p) atomic transition at 812.6 nm. The direct atomic fluorescence from the laser excited Li*($3p^2P$) state to the ground state is very weak due to heavy radiation trapping and it was experimentally difficult to resolve the atomic fluorescence from the scattered near-resonant pump laser light. We therefore chose to do the measurement indirectly, by monitoring the cascade fluorescence of the Li(3s−2p) atomic transition at 812.6 nm. The temporally integrated signal intensity is then measured as a function of detuning of the laser in the red and blue wings of the Li(2s−3p) transition. The closest state with energy below the Li(3p) asymptote other than the Li(3s) state is over 15 000 cm^{-1} away. For H_2 quenching where there is a possible electronic to vibrational or where rotational energy transfer is possible, neglecting the other states may not be a good enough approximation. We also believe in this experiment that the 3s state is predominantly populated through collisional quenching of the LiH_2, complex, even though we cannot rule out the possibility that the 3s state might also be populated by fluorescence from the Li(3p) state. However, the 3p−3s should be much less intense than the 3p−2s spontaneous emissions.

III. Experimental Results

The main experimental results of this work are presented in Figure 1. Figure 1a shows the relative population in the nonreactive product channel corresponding to process 1 in the red wing while Figure 1b shows similar result in the blue wing. In each case the signals are multiplied by Δ^2 in order to expand the scale and help visual enhancement of the weak far-wing signals. The profiles in each case are averaged over several runs and normalized to a constant incident energy.

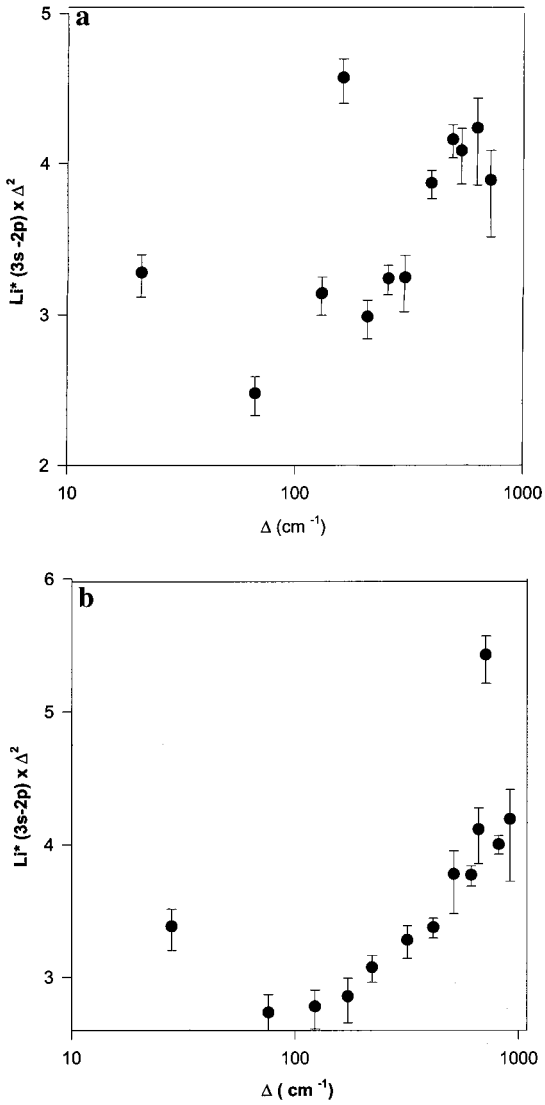

Figure 1. (a) A log−log plot of the experimental far-red-wing absorption profiles for (LiH_2) complex: Nonreactive Li(3s−2p) fluorescence signal as a function of pump laser detuning ($\Delta = \omega_L - \omega_o$) from Li(2s−3p) atomic resonance transition. The profiles have been multiplied by a factor Δ^2 (Δ is negative). (b) A log−log plot of the experimental far blue-wing absorption profiles for (LiH_2) complex: Nonreactive Li(3s−2p) fluorescence signal as a function of pump laser detuning ($\Delta = \omega_L - \omega_o$) from Li(2s−3p) atomic resonance transition. The profiles have been multiplied by a factor Δ^2.

A pronounced satellite is obvious in the blue-wing absorption spectra near $\Delta = 714$ cm^{-1}. The red-wing absorption spectra on the other hand appears to show a few more satellites, the strongest being at $\Delta = 162$ cm^{-1}.

In these experiments we have ruled out the possible influence of spontaneous emission in the far wing, and verified that the signals are linear in laser beam intensity and in H_2 pressure by measuring the signal at different values of H_2 pressure and incident laser power over the range of our operating conditions (see above).

IV. Computational Method

The atomic basis for lithium consists of 15s/10p/6d/3f Gaussian type orbitals used in a previous work[24] but these were used without contraction in this work. This basis can accurately

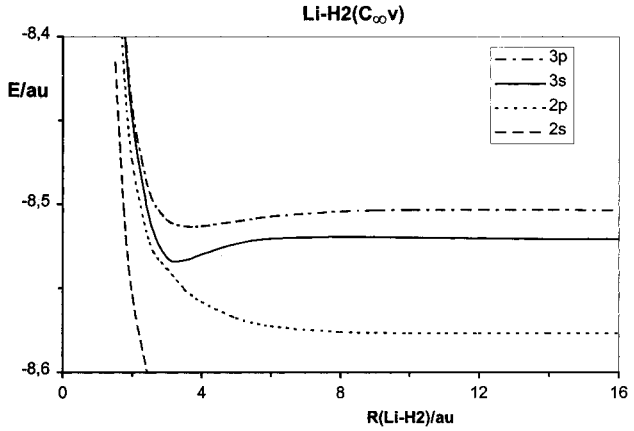

Figure 2. A linear section of the Li(2s), Li(2p), Li(3s), and Li(3p) potential energy surfaces showing the $^2\Sigma^+$ states where $R(\mathrm{H-H'}) = 1.4$ bohr.

describe all atomic states from 2s to 5p, Li^+ and Li^- as was shown before.[24] The atomic basis for hydrogen consists of 7s/3p/2d Gaussian type orbitals with exponents (19.79, 2.945, 0.7209, 0.2301, 0.08552, 0.031, 0.0098) for s, (1.4, 0.34, 0.093) for p, and (1.2, 0.25) for d. This gives the atomic energy of −0.499 71 hartree, and the electron affinity of 0.740 eV, which is quite close to the experimental value, 0.756 eV.[25] The bond energy of LiH calculated with this basis set is 19 992 cm^{-1}, which is quite close to the experimental value, 20 287.7 cm^{-1}.[26] This basis set is slightly better than that of ref 22 and we have done larger configuration interaction calculations for the LiH_2 system.

For each geometry, the multiconfiguration self-consistent-field calculations for all the electronic states correlated to the Li(2s−3p) were done to obtain the state-averaged molecular orbitals. Then the multireference configuration interactions were done with the active space including all molecular orbitals made from the σg and σu molecular orbitals of H_2 and the Li(2s−3p) atomic orbitals. All five electrons were allowed to make any combinations within the active space, and then all possible single-and-double substitutions from this zeroth wave function into all molecular orbitals were done. The dimension of the configuration state functions thus resulted was 1 112 569 for the $^2\Sigma^+$ state of linear ($C_{\infty v}$) geometry, 988 264 ($^2A_1$) and 905 991 ($^2B_2$) for the C_{2v} geometry, and 1 182 068 for the $^2A'$ irreducible representation of the C_s geometry. The MOLCAS program [27] was used for the molecular calculations. Such large configuration interactions ensure a high accuracy of the solutions. For example, the asymptotic energies calculated with different symmetries ($C_{\infty v}/C_s/C_{2v}$) are virtually identical.

V. Theoretical Results

The general geometry for the LiH_2 interaction is the C_s case. The $C_{\infty v}$ and C_{2v} geometries are only exceptional cases. The $Li + H_2 \rightarrow LiH + H$ reaction if ever happens should occur on the 2A′ potential surface. Figure 2 shows the $^2\Sigma^+$ states of a linear section of the $^2A'$ potential energy surfaces where the internuclear distance between the two hydrogen atoms, $R(\mathrm{H-H'})$, is 1.4 bohr. As the internuclear distance between the lithium atom and the hydrogen atom nearer to the lithium atom, $R(\mathrm{Li-H})$, is decreased (collision between Li and H_2), the 2p $^2\Sigma^+$ state is repulsive while the 3s $^2\Sigma^+$ and the 3p $^2\Sigma^+$ states are attractive leading to potential wells. The Li(2p) colliding with H_2 can make LiH product when the collision energy is large enough to compensate the endoergicity, 1624 cm^{-1}, as was explained in ref 22. This reaction occurs through a diabatic coupling between the 2 and 1 $^2A'$ states near the C_{2v} geometry. On the other hand, most of the Li(3s) colliding with H_2 undergoes a quenching to the Li(2p) state through a diabatic coupling between the 4 and 3 $^2A'$ states, as was explained in ref 22. Both the nonreactive Li(3s) + H_2 and the reactive Li(2p) + H_2 collsions have been recently confirmed by a reaction cell experiment of K.-C. Lin's team at Taipei. [28] Here we are going to have a closer look at this coupling.

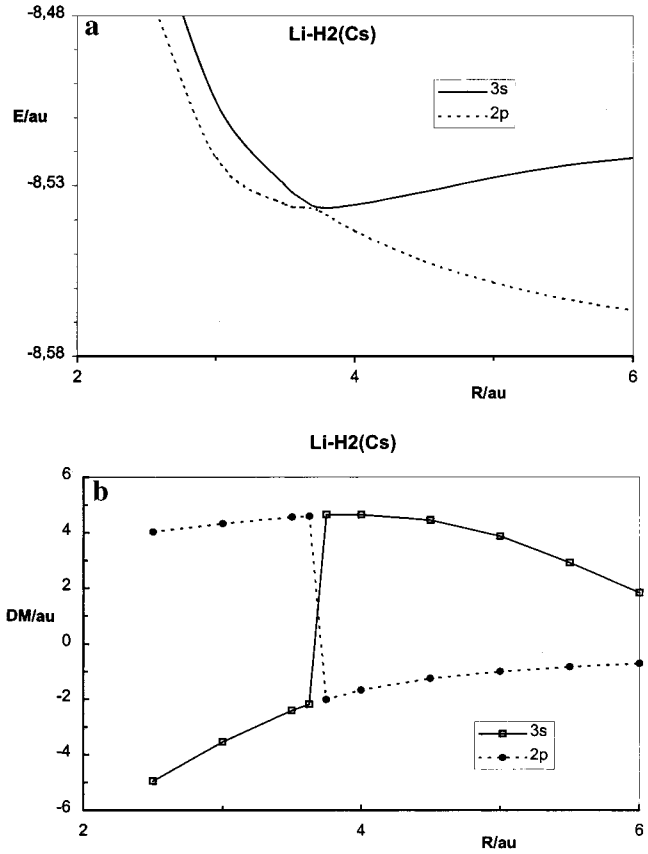

Figure 3. (a) A C_s section of the $3^2A'$ (2p) and $4^2A'$ potential energy surfaces with $R(\mathrm{H-H'}) = 1.5$ bohr and the hydrogen molecule making an angle of $\pi/4$ with the line connecting the midpoint of the hydrogen molecule and the lithium atom. [R in atomic units is the distance between Li and the midpoint of H_2]. (b) Dipole moments of the $3^2A'$ (2p) and $4^2A'$ states as functions of the $Li-H_2$ distance corresponding to Figure 2a. Positive values corresponds to $Li^+H_2^-$ and negative values corresponds to $Li^-H_2^+$. [R in atomic units is the distance between Li and the midpoint of H_2.]

Figure 3a shows a section of the 4 and 3 $^2A'$ potential energy surfaces with $R(\mathrm{H-H'}) = 1.5$ bohr (H is the hydrogen atom closer to the lithium atom and H′ is the hydrogen atom farther from the lithium atom) and the hydrogen molecule making an angle of $\pi/4$ with the line connecting the midpoint of the hydrogen molecule and the lithium atom. The avoided crossing between the $4^2A'$ and $3^2A'$ states is clearly shown in this figure. Analyzing other properties than the potential energy, for example the dipole moment, supports this avoided crossing, too. The dipole moments of these two adiabatic states corresponding to the section in Figure 3a are reported in Figure 3b. The avoided crossing appears very clearly in this figure. The 3s state has a dipole moment with $Li^+H_2^-$ while the 2p state has a dipole moment with $Li^-H_2^+$ at long distances. Their dipole moments are interchanged due to the avoided crossing around $R(H_2) \approx 3.7$ bohr.

The Li(3p) and Li(3s) initial states are closely coupled at short distances as can be seen in Figure 2 (linear geometry). This coupling is even closer in the C_{2v} geometry shown in Figure 4.

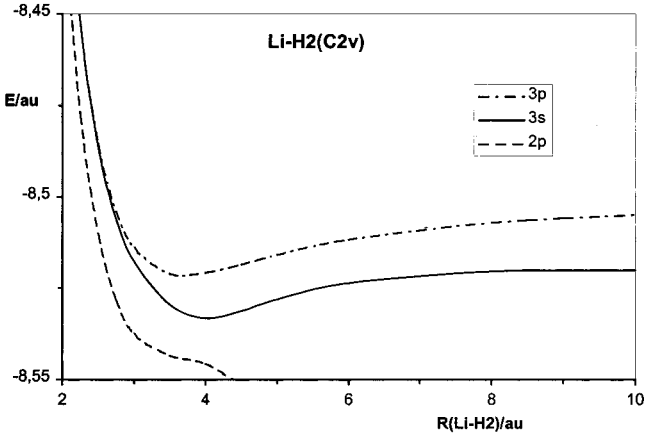

Figure 4. A C_{2v} section of the 3p($^2B_2$) and 3s($^2A_1$) potential energy surfaces with R(H−H) = 1.4 bohr.

TABLE 1: Crossing Line Segment between the 3p 2^2B_2 and 3s 4^2A_1 States (R in bohr and E in cm^{-1})

R(Li−H_2)	R_x(H−H)	E_x(cm^{-1})	R(Li−H_2)	R_x(H−H)	E_x(cm^{-1})
2.2	2.39	11512	3.3	1.73	−3659
2.3	2.41	7652	3.7	1.88	−3434
2.5	1.46	2164	4.1	1.95	−2292
2.7	1.50	−232	4.5	1.91	−1854
2.9	1.58	−3236	5.0	1.88	−2469
3.1	1.65	−3848			

The 3p−3s quenching occurs around the surface-crossing region between the 3^2A_1 and 2^2B_2 potential energy surfaces. Considering the two geometrical parameters of the C_{2v} geometry, R(Li−H_2) and R(H−H), the crossing forms a line segment often referred to as the "seam" line. The crossing geometries specified by R_x(Li−H_2) and R_x(H−H), and the crossing energies (E_x) of the seam line are tabulated in Table 1. This is only a part of the seam line, and to find the whole of the seam line would require investigation of a very wide range of geometry. The crossing energies are with respect to the Li + H_2 at infinity including the zero-point energy of H_2, 1873 cm^{-1}. For a given R(Li−H_2), the 2^2B_2 state is lower than the 3^2A_1 for the R(H−H) distance larger than the R_x(H−H), and vice versa. For the R(Li−H_2) less than about 2.2 bohr, the 3p($^2B_2$) state is lower than the 3s($^2A_1$) state. Theoretically, the surface transition (or hopping) probability of 3p−3s (or 3s−3p), p, at the seam line is 1. However, as the back transition 3s−3p (or 3p−3s, respectively) probability is also 1, the net transition for a single collision, $P = p(1 - p)$, along the seam line is zero. The largest net transition usually occurs near the crossing line. If too far from the seam line, the transition probability decreases rapidly (approximately inverse-exponentially proportional to the energy difference).

The lowest potential energy of Li(3p)H_2 is found in a C_{2v} geometry (the 2 $^2B_2$ state) with R(Li−H) = 3.79 bohr (201 pm) and R(H−H) = 1.48 bohr (78 pm). The binding energy of this state is 4103 cm^{-1} with respect to the Li(3p) + H_2. The corresponding spectroscopic data for the 1 $^2B_2$ state (Li(2p)H_2) are 170 pm, 83 pm, and 6780 cm^{-1}, respectively.[22] This shows Li(3p) makes significantly weaker binding with H_2 in comparison with Li(2p). The Li−H distance is also larger in the Li(3p)H_2 case than in the Li(2p)H_2 case. The H−H distance in Li(3p)H_2 is only slightly elongated from the free H_2 value, 74 pm, while it is significantly larger in the Li(2p)H_2 case.

VI. Discussion

The surface hopping rarely occurs in a single collision (the maximum transition probability is theoretically $^1/_4$ according to the above formula). The red-wing pumping excites the Li−H_2 complex to bound energy levels. The blue-wing pumping excites the complex to quasi-bound levels where the internal vibrations maintain the complex together but it will eventually split after a certain periods of vibration if no reaction or quenching takes place. The overall signal intensities are observed to be much higher in the red-wing than in the blue wing. This can be explained in terms of the lifetime of the excited states. As the red-wing states are stable states, they have lifetimes determined by the spontaneous emission rate, typically tens of nanoseconds. The blue-wing states have lifetime comparable to the vibrational period, H−H vibrational period being 18 fs. Even though the transition rate from one surface (3p) to another (3s, or vice versa) is of same order of magnitude, the longer lifetime of the red-wing states in comparison with the blue-wing states makes the quenching from the former state much larger than the latter. The red-wing (Δ being negative) quenching occurs mainly along the seam line in the negative side of energy in Table 1. More precisely, the neighborhood of the seam line segment below the red-shift energy contributes for quenching. For the blue-wing quenching case, the seam segment below the blue-shift energy (Δ being positive in Table 1) contributes where the neighborhood involves larger area than in the red-shift case.

The quenching of the Li(3s) to the Li(2p) was indirectly confirmed in a recent work by Lin's group at Taipei.[28] They have also observed production of LiH when the reaction is initiated from the Li(2p) with enough energy to overcome the endoergicity. A recent work by Vetter's group at Orsay [29] did not observe any trace of LiH when reaction is initiated by Li(3s) state. The present work is in agreement with these works.

We also measured the absorption profile of LiAr complex.[30] It shows a very similar profile to LiH_2 case in both the red and blue wings. This similarity may be explained in terms of a crossing of the attractive 3pΠ state and the repulsive part of the 3sΣ^+ state. Normally the diabatic transition does not occur between two states of different point-group symmetry, but the spin−orbit interaction allows mixing between these states with $\Omega = {}^1/_2$. Furthermore, although the spin−orbit coupling of Li is very small, the LiAr complex at short distance shows a large spin−orbit splitting originating from a mixture between the atomic orbitals of Li and Ar.[31] From a theoretical point of view, the spin−orbit interaction is a diabatic parameter in the LiAr case. It is the coupling between two $^2A'$ states (which is commonly called as the diabatic coupling) that makes a 3p−3s quenching in the LiH_2 case.

To understand the irregular quenching rate of the red-wing excitation would require a dynamical simulation involving a large area of the potential energy surfaces and the diabatic coupling matrix elements. This is not a scope of the present work. The blue-wing side shows a steady increase of the quenching rate as the detuning magnitude becomes large. This may be explained by the fact that the length of seam line participating in the diabatic transition process becomes longer as the higher states are populated. On the other hand, the transition probability for a given seam segment also increases (approximately exponentially) as the colliding kinetic energy increases. One datum in the blue wing (with Δ = 714 cm^{-1}) appears to be an exception. This energy state is believed to belong to a bound region made by a 3p potential barrier. The $^2\Sigma^+$ (linear) and $^2A_1$ (C_{2v}) states of 3p show a potential barrier originated from the atomic orbital structure found in a recent work.[23] The 3s state of LiH_2 also has been calculated to have a potential barrier[22] with the lowest height of 142 cm^{-1}. Our calculation for a limited area of the potential energy surfaces

showed the barrier height for 3p of about 100 cm^{-1}, so the real barrier height should be smaller than this. In contrast, the $^2B_2$ state does not have potential barrier due to the molecular orbital construction. Indeed, the 3p atomic orbital in this state is aligned parallel to the hydrogen molecular axis thus minimizing the steric repulsion. Considering a statistical averaging for different geometry, the single datum appearing in the blue-wing figure is expected to have a much longer lifetime in comparison with higher states, thus explaining higher quenching rate.

The harpooning model has been often used to explain the reaction mechanism of the alkali−dihydrogen reaction. As was explained before,[22] the charge transfer in the Li(2s), Li(2p), and Li(3s) + H_2 collision from the metal atom to the hydrogen molecule is very small, and nothing like a sudden transfer of one electron to the colliding partner occurs as in the metal−dihalogen cases. Figure 3b shows the case of Li(2p) and Li(3s) where no significant charge transfer occurs and the electron may be polarized from lithium toward hydrogen or from hydrogen toward lithium. (To get an appropriate charge transfer, divide the dipole moment by R(Li−H_2) in this figure.) The charge transfer from or into the lithium atom remains minor for the elongation/shortening of the interhydrogen distance. The harpooning model does not apply to the alkali−dihydrogen cases.

Our study showed the excitation of the lithium and H_2 mixture in gas-phase making the LiH_2 intermediate (red wing) or the transient complex (blue wing) which undergoes a rapid predissociation into Li*(3s) followed by the 3s−2p fluorescence. This result is consistent with the theoretical predictions. It also expalins the lack of reaction products at some point in the red wing.

Acknowledgment. We (S.B. and B.H.) gratefully acknowledge the financial support of the National Science Foundation (CHE 9733744 and CHE 9526197). The CNRS also has partially supported this work. Special thanks to Professor Thomas Sandin for kindly reading the manuscript.

References and Notes

(1) Breckenridge, W. H.; Umemoto, H. *Adv. Chem. Phys.* **1992**, *50*, 213.
(2) Krause, L. *Adv. Chem. Phys.* **1975**, *28*, 267.
(3) Nikitin, E. E. *Adv. Chem. Phys.* **1975**, *28*, 317.
(4) Gallagher, T. F.; Cooke, W. E.; Edelstein, S. A. *Phys. Rev.* **1978**, *A17*, 125.
(5) Hertel, V. *Adv. Chem. Phys.* **1982**, *50*, 475.
(6) Astruc, J. P.; Desfrancois, C.; Barbe, R.; Schermann, J. P. *J. Chem. Phys.* **1988**, *88*, 106.
(7) Lin, K. C.; Huang, C. T. *J. Chem. Phys.* 1989, **91**, 5387. Liu, D. K.; Chin. T. L.; Lin, K. C. *Phys. Rev.* **1994**, *A50*, 4891.
(8) Huang, X.; Zaho, J.; Xing, G.; Wang, X.; Bersohn. R. J. *J. Chem. Phys.* **1996**, *104*, 1338.
(9) L'Hermite, J.-M.; Rahmat, G.; Vetter, R. *J. Chem. Phys.* **1990**. 93, 434. L'Hermite, J.-M. *J. Chem. Phys.* **1992**, *97*, 6215.
(10) Fan, L.-H.; Chen, J.-J.; Lin, Y.-Y.;. Luh, W.-T. *J. Phys. Chem. A* **1999**, *103* (10), 1300; Chen, M.-L.; Lin, W.-C.; Luh, W.-T. *J. Chem. Phys.* **1997**, *106*, 5972.
(11) Kleiber, P. D. In *Chemical Dynamics and Kinetics of Small Radicals*; Liu, K., Wagner, A., Ed.; World Scientific: Singapore, 1996; Kleiber, P. D.; Stwalley, W. C.; Sando, K. M. *Annu. Rev. Phys. Chem.* **1993**, *44*, 13.
(12) Bililign, S.; Kleiber, P. D.; Kearney, W. R.; Sando, K. M. *J. Chem. Phys.* **1992**, *96*, 218.
(13) Bililign, S.; Kleiber, P. D. *J. Chem. Phys.* **1992**, *96*, 213.
(14) Kleiber, P. D.; Wong, T. H.; Bililign, S. *J. Chem. Phys.* **1993**, *98*, 1101.
(15) Wang, T.-H.; Kleiber, P. D.; Yang, K.-H. *J. Chem. Phys.* **1999**, *110*, 6743.
(16) Jenkins, D. R. *Proc. R. Soc. London Ser.* **1968**, *A306*, 413.
(17) Lin, S.-M.; Weston, Jr, R. E. *J. Chem. Phys.* **1976**, *65*, 1443.
(18) Berry, J. E.; Berry, M. J. *J. Chem. Phys.* **1980**, *72*, 4500.
(19) Myers, E. G.; Murnick, D. E.; Softky, W. R. *Appl. Phys.* **1987**, *B43*, 247.
(20) Yarkony, D. R. *Acc. Chem. Res.* **1998**, *31*, 511.
(21) Robinson, T. L. MS Thesis, North Carolina A&T State University, Greensboro, NC, 2000.
(22) Lee, H. S.; Lee, Y. S.; Jeung, G.-H. *J. Phys. Chem.* **1999**, *A103*, 11080.
(23) Bililign, S.; Hattaway, B. C., to be published.
(24) Yiannopoulou, A.; Jeung, G.-H.; Park, S. J.; Lee, H. S.; Lee, Y. S. *Phys. Rev.* **1999**, *A 59*, 1178.
(25) Peckeris, C. L. *Phys. Rev.* **1962**, *126*, 1470.
(26) Stwalley, W. C.; Zemke, W. T. *J. Phys. Chem. Ref. Data* **1993**, *22*, 87.
(27) A package of ab initio programs written by: Anderson, K.; Blomberg, M. R. A.; Fülscher, M. P.; Karlström, G.; Lindh, R.; Malmqvist, P.-A.; Neogrády, P.; Olsen, J.; Roos, B.; Sadlej, A. J.; Schütz, M.; Seijo, L.; Serrano-Andrés, L.; Siegbahn, P. E. M.; Widmark, P.-O. Lund University, Sweden 1997.
(28) Liu, D.-K.;. Lin, K.-C. A communication in: *French-Taiwanese Workshop: Dynamics and Spectroscopy of Metal/Molecule Reactions*; Taipei, Taiwan, 28 February−1 March 2000.
(29) Cavero-Manchado, V.; Luc, P.; Rahmat, G.; Vetter, R. Private Communication. Cavero-Manchado, V. Doctorate Thesis, Université de Paris-Sud, Orsay, 1997.
(30) Unpublished result.
(31) Park, S. J.; Lee, Y. S.; Jeung, G.-H. *Chem. Phys. Lett.* **2000**, *325*, 678.